PHYSICAL REVIEW C VOLUME 18, NUMBER 3 SEPTEMBER 1978

Neutron total cross section measurement on ^{140}Ce

H. S. Camarda
Lawrence Livermore Laboratory, University of California, Livermore, California 94550
(Received 3 April 1978)

A high resolution neutron time-of-flight experiment for neutron energies $20 \leq E \leq 240$ keV was carried out on the target nucleus ^{140}Ce(0^+). The measurement employed a 7.5 nsec beam burst and 250 m flight path. A multilevel shape analysis of the resonance data was performed. The plot of $\Sigma\Gamma_n^0$ vs E for the $l = 0$ $J^\pi = 1/2^+$ levels exhibited a significant change in slope at ~ 160 keV and gives support to the doorway state picture of compound nucleus formation. The observed number of $l = 0$ levels vs E showed an abrupt increase at 160 keV, the energy at which S_0 also changed. Various statistical tests were applied to see if this was an effect of missing weak levels but a definite conclusion could not be reached. The behavior of the p wave strength function vs energy was found to be suggestive of doorway state structure. After correcting for missing levels the ratio of s to p wave level spacings was found to be 3.0; the theoretical prediction of 2.9 (for $\sigma = 4.9$) is in good agreement with experiment. The average s, p strength functions and levels spacings are $S_0 = 1.1 \times 10^{-4}$, $S_1 = 0.34 \pm 0.05 \times 10^{-4}$, $\langle D \rangle_{l=0} = 4.9$ keV, $\langle D \rangle_{l=1} = 1.64$ keV.

[NUCLEAR REACTIONS Neutron total cross section measurement of ^{140}Ce, $20 < E < 240$ keV. Determined E, J^π, Γ_n of resonances. Deduced s and p wave strength functions and level spacings.]

INTRODUCTION

A high resolution neutron total cross section measurement on the separated isotope ^{140}Ce has been carried out for incident neutron energies $20 \leq E \leq 240$ keV. These results are part of an investigation of the neutron resonance behavior of a few closed shell nuclei for which current experimental technique can resolve a statistically significant number of levels over a several hundred keV energy region. Fewer degrees of freedom are excited in closed shell nuclei and consequently they represent favorable test cases for exhibiting the effects of isolated doorway states.[1] The doorway state signature of interest is an energy modulation of the s or p wave neutron strength function which is more rapid than that predicted by the optical model.[2] A previously reported result on ^{89}Y (Ref. 3) gave evidence in favor of the doorway state picture and provided impetus for the ^{140}Ce measurement. Furthermore, as was the case for ^{89}Y (see Ref. 3) most s and p levels were detected and this lends itself to a good test of the expected ratio of s to p wave level spacings.

^{140}Ce is a 0^+ closed shell nucleus ($N = 82$) and lies on the low A side of the split $4S$ maximum in the s wave strength function. The behavior of the p wave strength function in the $A = 140$ region is unclear because little reliable data exist.

EXPERIMENT

The experiment was carried out with basically the same set up as described in Ref. 3. The 100 MeV electron beam from the Lawrence Livermore Laboratory linear accelerator struck a water cooled neutron producing Ta target which was viewed by three 1 cm thick, 12.7 cm diam, ^{6}Li glass scintillators located at the end of a 250 m evacuated flight tube. An important difference between the ^{140}Ce and ^{89}Y measurement is that the plastic adapters used to couple the flat Li glass scintillators to the phototubes were replaced by quartz adapters. As described in Ref. 3, this improved the resolution. The accelerator was operated at 720 pps with a 7.5 nsec beam width and an average electron current of 25 μA. The time-of-flight tehnique was used and below (above) 180 keV 4 nsec (2 nsec) channel widths were employed, respectively. The effective resolution was satisfactorily described by a time smearing of 12 nsec and was found to vary little with neutron energy.

The separated isotope ^{140}Ce was in the chemical form CeO_2 and consisted of 99.7% (at.%) ^{140}Ce. The 388 g of ^{140}Ce (476 g of CeO_2) was contained in an Al cylinder 5.8 cm in diam. resulting in a ^{140}Ce sample thickness of $1/n = 16.1$ b/atom. An equivalent Al container was in the open beam. Fast cycling determined the normalization between open and sample runs and backgrounds at 28 and 80 keV were determined using Fe filters. Further experimental details are described in Ref. 3.

ANALYSIS

The ^{140}Ce data were analyzed with a multilevel shape analysis program which was written in the process of analyzing the ^{89}Y data of Ref. 3. The

theoretical cross section, which included the effects of Doppler broadening, was represented by an incoherent sum of $l=0$ and $l=1$ Breit-Wigner equations. These equations do not correctly treat coherent interference between resonances with the same quantum numbers but this is only important if these levels have significant overlap—which seldom occurs. The exact equations used are

$$\sigma_t = \sigma_0 + \sigma_1 , \tag{1a}$$

$$\sigma_0 = 4\pi\chi^2 \sum_J [g_J(\Gamma_n^s)_J/\Gamma_J^s]\cos 2\gamma_0 \times [\psi(B_J, X_J) + \tan 2\gamma_0 \chi(B_J, X_j)] + 4\pi\chi^2 \sin^2\gamma_0 , \tag{1b}$$

$$\sigma_1 = 4\pi\chi^2 \sum_J [g_J(\Gamma_n^P)_J/\Gamma_J^P]\cos 2\gamma_1 \psi(B_J, X_J) + 4\pi\chi^2(3\sin^2\gamma_1) , \tag{1c}$$

$$\Gamma_n^s = [E/(1\text{ eV})]^{1/2}\Gamma_n^0 , \tag{1d}$$

$$\Gamma_n^P = [E/(1\text{ eV})]^{1/2}[y^2/(1+y^2)]\,\Gamma_n^1 , \quad y = kR , \tag{1e}$$

$$\Gamma = \Gamma_n + \Gamma_\gamma , \tag{1f}$$

$$X_J = 2(E - E_J)/\Gamma_J , \tag{1g}$$

$$B = 2\Delta/\Gamma , \quad \Delta = (E/10A)^{1/2} , \tag{1h}$$

$$\gamma_0 = kR' , \quad R' = R(1 - R_0^\infty) , \tag{1i}$$

$$\gamma_1 = \phi_1 + \theta_1 , \tag{1j}$$

$$\phi_1 = \tan^{-1}[-j_1(y)/\eta_1(y)] , \tag{1k}$$

$$\theta_1 = \tan^{-1}[-R_1^\infty P_1/(1 - R_1^\infty S_1)] , \tag{1l}$$

$$P_1 = y^3/(1+y^2), \quad S_1 = y^2/(1+y^2) . \tag{1m}$$

The definitions of the different parameters and the form of cross section above result from an R-matrix[4] derivation of the Breit-Wigner equation. σ_0 and σ_1 give the s and p wave contribution to the total cross section. Γ_n, Γ_γ, E_J, and g_J are the neutron width, capture width (assumed to be 0.1 eV for all levels), resonance energy, and spin factor associated with each level. For the $l=1$ case a self-interference term similar to the $l=0$ term $[\sin 2\gamma_0\chi(B_J, X_J)]$ was not included because it is not important for the neutron energies covered in this experiment. For ^{140}Ce the nuclear radius R was taken to be 7.26 fm and gave a best estimate of $R_0^\infty = 0.3 \pm 0.05$ ($R' = 5.1 \pm 0.3$ fm). The value of R_0^∞ is in good agreement with previous measurements in this mass region.[5] $\psi(B,X)$ and $\chi(B,X)$ are the Doppler broadening integrals which replace $1/(1+X^2)$ and $X/(1+X^2)$ in the usual Breit-Wigner equation. The experimentally observed transmission was calculated by convoluting the transmission $T = \exp(-n\sigma_t)$ with a resolution function which was determined by examining narrow levels. Figure 1 shows the experimental transmission (data points) vs neutron energy for $^{140}CeO_2$. The oxygen total cross section is constant for $E \leq 240$ keV and was taken to be 3.76 b.[6] Thus the smooth curve through the data includes the transmission of oxygen in addition to the multilevel cross section of ^{140}Ce as described above.

As can be seen from the data of Fig. 1 the $l=0$ levels are easily identified by their interference minimum and are $\frac{1}{2}^+$ resonances. Symmetric resonances were assumed to be p wave and for these levels only $g\Gamma_n$ could be determined. The good resolution of this experiment enabled the parity of many weak levels to be determined unambiguously. For example, the resonances at 30.698 and 108.10 keV have small widths but their s wave character is obvious without any shape fitting of the data. For the resonance at 205.69 keV where the resolution, though still good, is poorer the shape analysis clearly gives a superior fit when $l=0$ is assumed for the resonance.

Tables I and II list the $l=0$ and $l=1$ resonance parameters, respectively. The symbol † next to the 213.98 keV resonance in Table I signifies a multiple level, while the * adjacent to the 10 weak levels in Table II indicates the parity could not be determined by the shape analysis. These levels were placed in Table II because a Bayes theory test[7] indicates $\geq 85\%$ probability of these levels being p wave (it is reasonable to assume that two or three of these levels are s wave). The only other measurement on ^{140}Ce that this author is aware of is unpublished work performed by the Columbia group.[8] Their results covered the energy range $E \lesssim 60$ keV and the two sets of values of the $l=0$ resonance parameters are in good agreement.

RESULTS

Figure 2 shows the behavior of $\sum\Gamma_n^0$ vs E for the $l=0$ $\frac{1}{2}^+$ levels. The slope of the data yields the s wave neutron strength function which should be essentially constant over this energy range if the optical potential provided a complete description of the neutron nucleus interaction. As can be seen the data of Fig. 2 cannot be characterized as having a constant slope and hence an energy independent $l=0$ strength function S_0. Beyond the strong 21.57 keV level, which produces an immediate rise in $\sum\Gamma_n^0$, S_0 naturally (not forced) follows two different slopes below and above a neutron energy of 160 keV. The straight lines drawn through the data are meant to emphasize this behavior and are not fits to the data. Attempts at drawing a straight line through all the data, i.e., including the 21.57

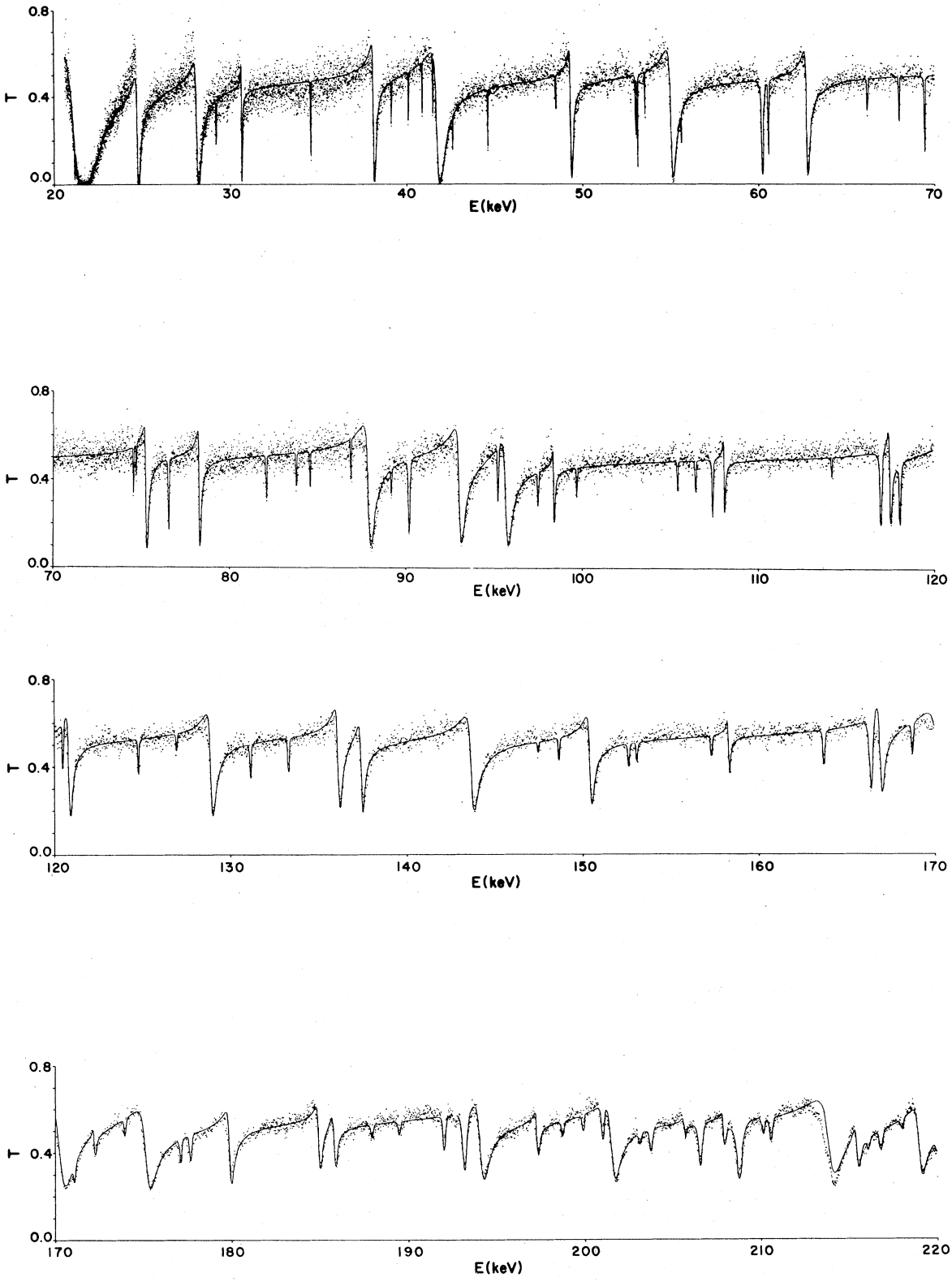

FIG. 1. (a), (b) Transmission vs neutron energy of $^{140}CeO_2$ ($1/n$ value of $^{140}Ce = 16.1$ b/atom). The smooth curve through the data results from a multilevel fit as described in the text.

TABLE I. $l = 0$ resonance parameters of ^{140}Ce.

E (keV)	Γ_n (eV)
21.570 ± 0.010	550 ± 60
24.795 ± 0.006	73 ± 10
28.190 ± 0.008	110 ± 15
30.698 ± 0.008	11.6 ± 2.5
38.175 ± 0.010	75 ± 10
41.870 ± 0.010	260 ± 30
49.390 ± 0.010	65 ± 10
55.130 ± 0.015	190 ± 25
62.810 ± 0.020	120 ± 15
73.300 ± 0.020	95 ± 15
78.300 ± 0.020	75 ± 10
87.950 ± 0.030	290 ± 35
93.090 ± 0.030	270 ± 35
95.740 ± 0.030	280 ± 35
98.400 ± 0.020	33 ± 5
108.10 ± 0.02	28 ± 5
117.53 ± 0.03	75 ± 15
120.89 ± 0.03	170 ± 20
128.96 ± 0.03	265 ± 30
136.16 ± 0.03	195 ± 25
137.46 ± 0.03	150 ± 25
143.77 ± 0.04	380 ± 35
150.48 ± 0.04	220 ± 30
158.34 ± 0.03	40 ± 5
166.96 ± 0.04	200 ± 30
170.40 ± 0.05	800 ± 100
172.23 ± 0.04	25 ± 4
175.25 ± 0.04	600 ± 60
179.92 ± 0.06	230 ± 40
184.97 ± 0.03	120 ± 20
185.84 ± 0.03	80 ± 15
194.17 ± 0.04	485 ± 55
197.32 ± 0.03	65 ± 15
201.63 ± 0.03	500 ± 70
205.69 ± 0.04	22 ± 5
207.90 ± 0.04	42 ± 8
† 213.98 ± 0.09	800 ± 200
215.49 ± 0.04	95 ± 15
219.05 ± 0.04	400 ± 60
224.45 ± 0.04	480 ± 60
228.55 ± 0.05	40 ± 8
235.49 ± 0.05	500 ± 70

keV resonance, does not satisfactorily represent the energy dependence of S_0. The data of Fig. 2 gives clear evidence of a change in slope at a neutron energy of 160 keV and is typical of the behavior expected (see Ref. 3) if an isolated doorway state with a spreading width $\Gamma^{\downarrow} \sim 100$ keV modulated the strength of the interaction. A *representative* value of the s wave strength function in this energy range is 1.1×10^{-4}.

Figure 3 displays $\sum g\Gamma_n^1$ vs energy for p wave levels of both spins ($\frac{1}{2}^-$ and $\frac{3}{2}^-$). The solid and broken lines through the data represent two possible interpretations of the energy dependence of

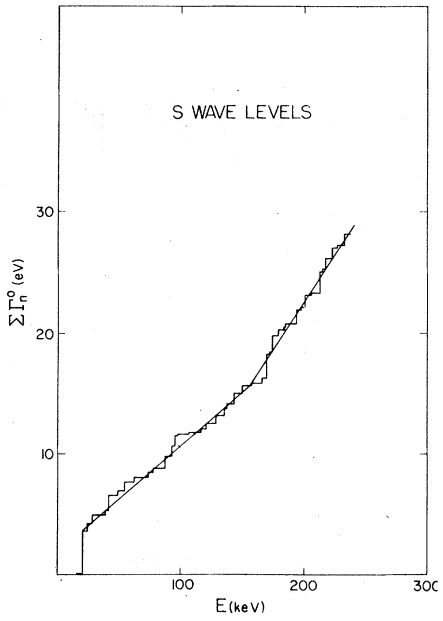

FIG. 2. Plot of $\sum \Gamma_n^0$ vs neutron energy for the $l = 0$ $J = \frac{1}{2}^+$ levels. The straight lines through the data were drawn to emphasize the different slopes above and below 160 keV. A *representative* value of the s wave strength function over the 20 to 240 keV region is 1.1×10^{-4}.

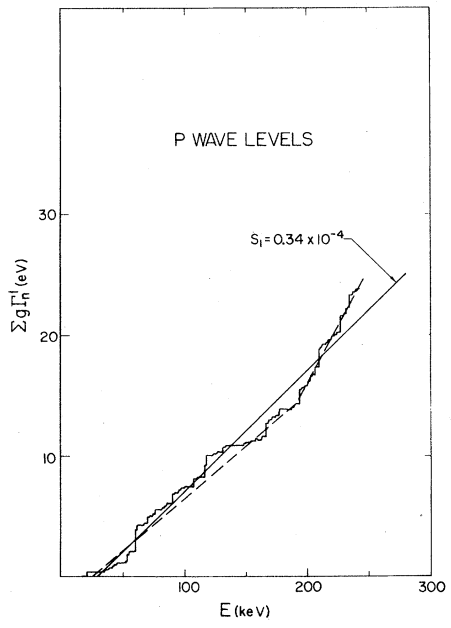

FIG. 3. Plot of $\sum g\,\Gamma_n^1$ vs neutron energy for the p wave resonances of both spin states, $\frac{1}{2}^-$ and $\frac{3}{2}^-$. The solid and broken lines drawn through the data are discussed in the text.

TABLE II. $l = 1$ resonance parameters of ^{140}Ce. Levels with symbol * are of undetermined parity but a Bayes theory test (see text) indicates that these are most likely p wave.

	E (keV)	$g\Gamma_n$ (eV)		E (keV)	$g\Gamma_n$ (eV)
*	21.183 ± 0.004	2.0 ± 0.5		133.32 ± 0.02	21 ± 3
	29.200 ± 0.004	0.8 ± 0.2		147.50 ± 0.04	5 ± 2.5
	34.575 ± 0.006	2.7 ± 0.4	*	148.68 ± 0.03	13 ± 2.5
	39.145 ± 0.007	1.3 ± 0.2		152.64 ± 0.03	18 ± 3
	40.108 ± 0.007	1.5 ± 0.2		153.12 ± 0.03	14 ± 3
	40.890 ± 0.007	1.5 ± 0.2		157.35 ± 0.03	14 ± 3
	41.495 ± 0.007	1.7 ± 0.3		163.75 ± 0.03	30 ± 4
	42.620 ± 0.007	2.0 ± 0.4		166.42 ± 0.04	140 ± 30
	44.620 ± 0.008	2.9 ± 0.4		168.76 ± 0.04	25 ± 7
	48.510 ± 0.008	1.5 ± 0.3		171.08 ± 0.04	30 ± 7
	53.050 ± 0.010	3.5 ± 0.7		173.95 ± 0.05	15 ± 4
	53.150 ± 0.010	15 ± 3		177.10 ± 0.04	30 ± 4
	53.580 ± 0.010	2.2 ± 0.3		177.65 ± 0.04	35 ± 4
	55.615 ± 0.011	3.0 ± 0.4		187.94 ± 0.04	15 ± 3
	60.255 ± 0.011	60 ± 8		189.49 ± 0.04	15 ± 3
	60.600 ± 0.011	14 ± 3		192.03 ± 0.04	50 ± 7
	66.210 ± 0.015	3.3 ± 0.5		193.19 ± 0.04	175 ± 25
	68.025 ± 0.013	5.4 ± 0.8		198.74 ± 0.04	20 ± 4
	69.475 ± 0.012	18 ± 3		199.92 ± 0.05	18 ± 5
	74.560 ± 0.020	6 ± 2.5		201.04 ± 0.04	55 ± 8
*	74.725 ± 0.020	3.3 ± 1.0	*	203.14 ± 0.04	15 ± 5
	76.555 ± 0.015	18 ± 3		203.78 ± 0.04	40 ± 5
	82.100 ± 0.020	9.0 ± 1.3		206.57 ± 0.04	110 ± 15
*	83.795 ± 0.025	6.0 ± 1.0		208.78 ± 0.04	250 ± 35
*	84.575 ± 0.025	6.0 ± 1.0		210.16 ± 0.05	22 ± 5
*	86.880 ± 0.030	7.0 ± 2.0		210.59 ± 0.05	38 ± 6
	89.167 ± 0.030	5.0 ± 1.0		216.10 ± 0.05	20 ± 7
	90.180 ± 0.020	40 ± 5		216.82 ± 0.05	35 ± 5
	95.230 ± 0.020	18 ± 3		218.04 ± 0.05	13 ± 4
	97.495 ± 0.020	12 ± 3		220.10 ± 0.05	35 ± 5
	99.685 ± 0.025	9 ± 1.5		221.98 ± 0.05	35 ± 5
	105.44 ± 0.02	8 ± 1.5		225.13 ± 0.05	17 ± 4
	106.46 ± 0.02	9 ± 1.5		226.11 ± 0.05	20 ± 5
	107.43 ± 0.02	30 ± 4		227.14 ± 0.05	240 ± 30
*	114.23 ± 0.03	6 ± 1.5	*	231.68 ± 0.05	15 ± 5
	117.00 ± 0.02	70 ± 9		232.15 ± 0.05	47 ± 10
	118.08 ± 0.02	50 ± 8		232.60 ± 0.05	40 ± 7
	120.52 ± 0.03	20 ± 4		233.19 ± 0.05	30 ± 7
	124.79 ± 0.02	15 ± 2		234.86 ± 0.05	170 ± 25
*	126.95 ± 0.03	6 ± 1.5		236.97 ± 0.05	20 ± 4
	131.16 ± 0.02	22 ± 3		238.65 ± 0.05	25 ± 4

the p wave strength function S_1. The solid line demonstrates how a straight line can be found which gives a reasonable fit to the data up to about 220 keV. The p wave data above ~220 keV does have a steeper slope; however, higher energy data are required to see if this trend continues. It is also possible to separate the p wave data into regions with different slopes below and above 190 keV, which implies an energy dependence of S_1. This is shown by the broken lines through the data of Fig. 3. It is felt that the evidence for a doorway state in the p wave channel is weaker than the s wave case. A better test of doorway states in the p wave channel requires identifying the J values of the resonances in order that the $\frac{1}{2}^-$ and $\frac{3}{2}^-$ channels be examined separately. The straight line through the p wave data gives a p wave strength function of $S_1 = 0.34 \times 10^{-4}$. The statistical uncertainty is estimated to be ± 0.05.

The cumulative number of s levels vs energy is plotted in Fig. 4. This plot is rather startling in that two different level densities are implied below and above 160 keV. They are 5.9 and 4.0 keV, respectively. It is tempting to claim that the true s wave level density has changed at the same energy at which the strength function changed. How-

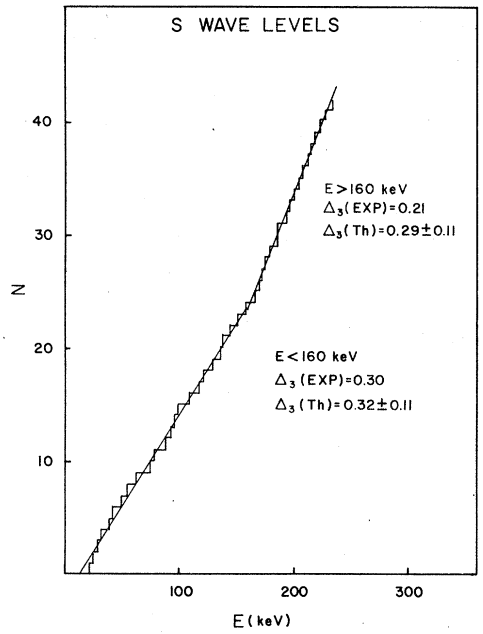

FIG. 4. Plot of the cumulative number of s wave levels vs neutron energy. The straight lines were drawn to emphasize the different slopes below and above 160 keV. The expected values of the Dyson-Mehta Δ_3 statistic, along with the experimental values, are also presented.

ever, as usual, one always has the problem of estimating how many weak s levels were missed. Between 20 and 160 keV 24 s levels were observed while above 160 keV 18 resonances were detected. If it is assumed [see Fig. 5(b)] that no s levels were missed above 160 keV it is necessary to include 11 additional levels between 20 and 160 keV to bring the different $\langle D \rangle$ values into agreement. The histograms of Figs. 5(a) and 5(b) represent the experimental distribution of $l=0$ reduced neutron widths for the energy region below and above 160 keV. The smooth curve of Fig. 5(b) represents the Porter-Thomas[9] (PT) distribution and represents the expected distribution when the total number of widths equals 18. The agreement between the histogram and the PT curve suggests there are few missing levels. The smooth curves of Fig. 5(a) were calculated assuming a total of 24 (observed) and 35 (missing 11) levels. Since the first hisotgram box of Fig. 5(a) shows to few counts it might seem reasonable to conclude that many small resonances are being missed below 160 keV. There are, however, two other factors to consider. Firstly, the experimental resolution is better at lower energies even if one concludes, as is implied by a constant $\langle D \rangle$ and the increased strength function, that the reduced neutron widths above 160 keV are larger. Secondly, the Dyson-Mehta[10] Δ_3 statistic is expected to have the value

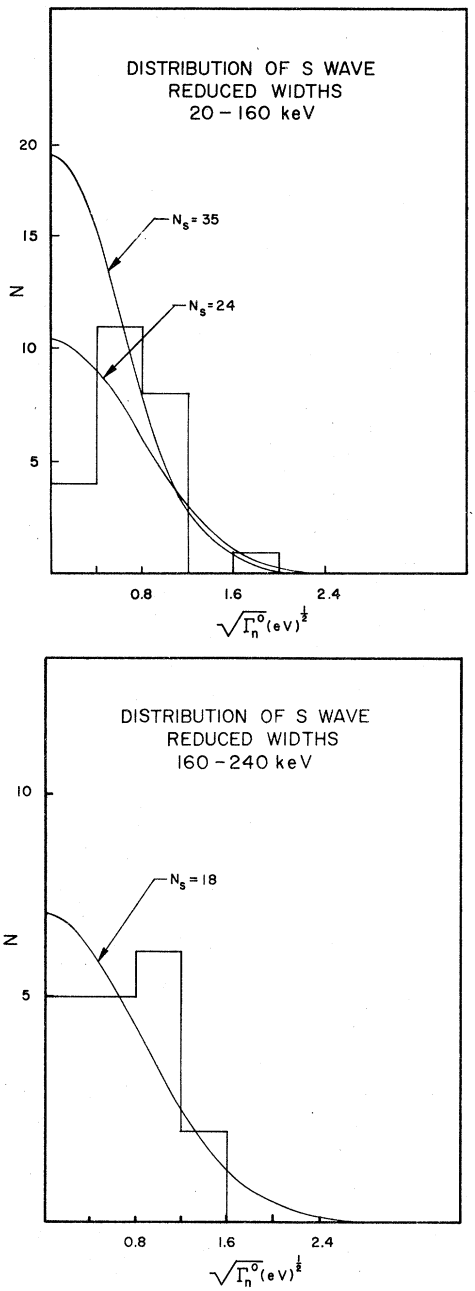

FIG. 5. (a), (b) The histograms represent the experimental distributions of reduced $l=0$ neutron widths. The smooth curves represents the Porter-Thomas distribution for the assumed number of true levels.

0.315 ± 0.11 for a sequence of 24 correlated levels. The experimental value of Δ_3 found for the 24 levels between 20 and 160 keV is 0.30. Since the value of Δ_3 tends to be larger than expected when levels are missed,[11] the "good" value of Δ_3 found experimentally suggests only a few levels have been missed.

In order to be more quantitative two Monte

Carlo calculations were performed. The first calculation centers around the PT distribution. Assuming that the true number of s levels below 160 keV is the 24 observed, the probability of finding ≤ 4 "counts" in the first histogram box [see Fig. 5(a)] was determined. It was found to be between 1 and 2%. The second calculation employed the Δ_3 statistic as a test of missing levels. Here it was assumed that the true number of levels below 160 keV is 35 and the question is as follows: What is the probability of missing 11 levels and finding a value of $\Delta_3 \leq 0.30$? This was determined as follows: A sequence of 35 levels having $\Delta_3 = 0.36$ (close to the expected value of 0.35) was selected. Eleven levels were randomly chosen to be missing and for the remaining 24 levels a value of Δ_3 was calculated. This process was repeated many times and the probability of having $\Delta_3 \leq 0.30$ for the remaining 24 levels was found to be between 4 and 5%.

As these tests imply opposite conclusions with about equal weight a definite interpretation of the change in $\langle D \rangle$ cannot be made conclusive. On the other hand, it is interesting to note that a change in level density, occurring at the same energy at which the $l=0$ strength function exhibited a change, was reported recently for ^{203}Tl by Liou *et al.*[12] This favors concluding that a true change in $\langle D \rangle$ is being observed in ^{140}Ce. It should be pointed out that a simultaneous change in S_0 and $\langle D \rangle$ is contrary to the doorway state picture of the neutron nucleus interaction. A doorway state is expected to modulate the strength of the resonances but not their average spacing.

With the data collected in this experiment it is possible to examine the expected ratio of s to p wave level spacing about which little information exists. It will be assumed that few $l=0$ resonances have been missed even though, as discussed above, this may not be true. Since the Bayes theory test described previously implies that several weak levels assigned to be $l=1$ might be $l=0$, the total number of s wave levels between 20 and 240 keV was taken to be 45 (3 more than the observed 42). This gives an average spacing of $\langle D \rangle_{l=0} = 4.9$ keV.

Before determining the p wave resonance spacing the number of missing weak levels must be determined. This was done by looking for satisfactory agreement between the expected and observed distribution of widths while varying the true number of p wave levels. Specifically, the expected distribution of $\frac{1}{2}^-$ and $\frac{3}{2}^-$ p wave reduced widths has the form:

$$P(\chi)\,d\chi = \tfrac{1}{3}N_P[P_{1/2}(\chi) + 2P_{3/2}(\chi)]\,d\chi, \quad \chi = (g\Gamma_n^1)^{1/2}, \tag{2a}$$

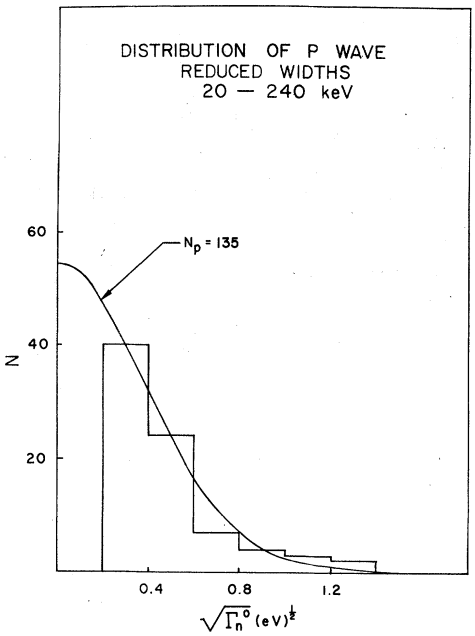

FIG. 6. The histogram gives the experimental distribution of reduced $l=1$ neutron widths and the smooth curve represents the expected distribution as described in the text.

$$R = \langle g\Gamma_n^1 \rangle_{3/2} / \langle g\Gamma_n^1 \rangle_{1/2}, \tag{2b}$$

$$\langle g\Gamma n^1 \rangle_{3/2} = \frac{9S_1\Delta E}{N_P} \frac{R}{2R+1}. \tag{2c}$$

S_1 is the measured strength function (both spins) equal to 0.34 for the energy interval $\Delta E = 220$ keV and R is the ratio of the $p_{3/2}$ to $p_{1/2}$ strength functions which an optical model calculation[5] indicates is 0.6 in the $A = 140$ region. $P_{1/2}$ and $P_{3/2}$ are the probability distributions for the $J = \frac{1}{2}$ and $\frac{3}{2}$ p wave levels. The only free parameter is N_P the true number of p levels. In Fig. 6 the histogram represents the experimental distribution of reduced $l=1$ widths and the smooth curve was calculated using Eq. (2) with $N_P = 135$ (53 more than the 82 observed). The fit to the data is satisfactory and 135 p wave levels implies $\langle D \rangle_{l=1} = 1.64$ keV. Thus the "experimental value" of $\langle D \rangle_{l=0} / \langle D \rangle_{l=1} = 3$.

Thermodynamic level density calculations[13] predict a J dependence (for either parity) of the form $(2J+1)\exp -(J+\frac{1}{2})^2/2\sigma^2$ where σ = spin cutoff factor. For $\sigma = \infty$ the expected ratio of $\langle D \rangle_{l=0} / \langle D \rangle_{l=1}$ is 3 while for $\sigma = 4.9$, which is typical of the $A = 140$ region, the expected ratio is 2.9. The agreement between theory and experiment is satisfactory.

*Work performed under the auspices of the U. S. Energy Research and Development Administration, W-7405-Eng-48.

[1]H. Feshbach, A. K. Kerman, and R. H. Lemmer, Ann. Phys. (N.Y.) 41, 230 (1967).
[2]H. Feshbach, C. Porter, and V. F. Weisskopf, Phys. Rev. 96, 448 (1954).
[3]H. S. Camarda, Phys. Rev. C 16, 1803 (1977).
[4]A. M. Lane and R. G. Thomas, Rev. Mod. Phys. 30, 257 (1958).
[5]H. S. Camarda, Phys. Rev. C 9, 28 (1974).
[6]*Resonance Parameters*, compiled by S. F. Mughabghab and D. I. Garber, Brookhaven National Laboratory Report No. 325 (National Technical Information Service, Springfield, Virginia, 1973), 3rd ed., Vol. 1.
[7]L. M. Bollinger and G. E. Thomas, Phys. Rev. 171, 1293 (1968).
[8]J. Rainwater (private communication).
[9]C. E. Porter and R. G. Thomas, Phys. Rev. 104, 483 (1956).
[10]F. Dyson and M. L. Mehta, J. Math. Phys. 4, 701 (1963).
[11]H. I. Liou, H. S. Camarda, and F. Rahn, Phys. Rev. C 5, 1002 (1972).
[12]H. I. Liou, J. Rainwater, G. Hacken, and U. N. Singh, Phys. Rev. C 12, 102 (1975).
[13]A. Gilbert and A. G. W. Cameron, Can. J. Phys. 43, 1446 (1965).